



# CHEMISTRY & BIOLOGY INTERFACE

An official Journal of ISCB, Journal homepage; [www.cbijournal.com](http://www.cbijournal.com)

## Synthesis, anti-microbial evaluation and molecular docking studies of some novel tetrazole containing azodye derivatives

Bhaurao P. Sathe,<sup>a</sup> Pramod S. Phatak,<sup>a</sup> Naziya N. M. A. Rehman,<sup>b</sup> Prashant P. Dixit,<sup>b</sup> Vijay M. Khedkar,<sup>c</sup> Suresh G. Vedpathak,<sup>d</sup> Kishan P. Haval<sup>\*†</sup>

<sup>a</sup>Department of Chemistry, Dr. Babasaheb Ambedkar Marathwada University, SubCampus, Osmanabad-413501, Maharashtra, India

<sup>b</sup>Department of Microbiology, Dr. Babasaheb Ambedkar Marathwada University, SubCampus, Osmanabad-413501, Maharashtra, India

<sup>c</sup>Department of Pharmaceutical Chemistry, Shri Vile Parle Kelavani Mandal's Institute of Pharmacy, Mumbai - Agra National Hwy, Dhule-424001 Maharashtra, India.

<sup>d</sup>Department of Chemistry, S. M. D. M. College, Kallam-413507, Dist. Osmanabad, Maharashtra, India

\*Corresponding author. Tel: +919423531375 E-mail: [havalkp@gmail.com](mailto:havalkp@gmail.com)

Received 28 November 2018, Accepted 3 April 2019

**Abstract:** In the present study, a series of novel tetrazole containing azodye derivatives were synthesized for first time. An optimized reaction condition was established for this purpose. The diazotization of 1, 5-disubstituted tetrazole containing amines in presence of  $\text{Fe}_3\text{O}_4@\text{SiO}_2\text{-SO}_3\text{H}$  solid acid catalyst followed by coupling reaction furnished the corresponding azodyes derivatives. The structures of the compounds were characterized by  $^1\text{H}$  NMR and  $^{13}\text{C}$  NMR spectra. All the synthesized compounds were evaluated for their antimicrobial activities. Several of these compounds shows very excellent to reasonable anti-microbial activities against *Staphylococcus aureus*, *Bacillus cereus*, *Bacillus megaterium*, *Micrococcus glutamicum*, *Bacillus subtilis* etc. We further performed exploratory docking studies on microbial DNA gyrase to rationalize the in vitro-biological data and to demonstrate the mechanism of antimicrobial activities in which some compounds displayed best anti-microbial activities among the synthesized compounds.

**Keywords:** Tetrazole, Azodye, One-pot synthesis, Diazo-coupling reaction, Antimicrobial and Docking study.

### 1. Introduction

The frequency of microbial infections is increasing globally even though vigorous research devoted to the discovery and development of

novel antimicrobial agents.[1] The problem of drug resistance increased dramatically due to appearance of multiresistant strains of bacteria.[2] Various attempts were carried out to the current existing drugs for reducing the

microbial resistance.[3] The literature survey reveals that tetrazole containing azodyes derivatives have been reported [4] and possess antimicrobial activity.[5] Tetrazole derivatives are well known compounds for possessing high level of biological activities [6]. It includes antiviral, antibacterial, antifungal, antiallergic, anticonvulsant and anti-inflammatory properties [7]. Recently, Popova et. al. and others [8] reported new tetrazole derivatives as promising compounds for anticancer activity. Tetrazoles have also found a wide range of applications in explosives, photography and information recording systems [9]. They are precursors for a variety of nitrogen containing heterocyclic compounds [10]. It exhibit stronger resistance to *in vivo* metabolization than the carboxylate group, thus conferring to the corresponding drug longer lifetimes (bioavailability) in blood [11]. Owing to their wide importance, much attention is being paid to the tetrazole containing heterocyclic compounds [12]. Azodyes play a major role in textile, printing, leather, papermaking, drug and food industries [13]. However, very few heterocyclic azodyes are reported in literature having antimicrobial and antioxidant activities [14]. In the present study, we have synthesized tetrazole containing azodye derivatives. In addition, antimicrobial activity and docking study of newly synthesized compounds is reported.

## 2. Materials and Methods

### 2.1 General

All reagents were purchased from Merck and Aldrich and used without further purification. Melting points were determined in open capillaries and are uncorrected.  $^1\text{H}$  and  $^{13}\text{C}$  NMR spectra were recorded on a Bruker 400 MHz and 100 MHz spectrometer respectively.

### 2.2. General procedure for the preparation of tetrazole containing azodye derivative.

Substituted tetrazole amine (20 mmol),  $\text{Fe}_3\text{O}_4@\text{SiO}_2\text{-SO}_3\text{H}$  MNPs (20 mol%) and sodium nitrite (40 mmol) were grinded in a mortar with a pestle for a few minutes. Then, a few drop of water was gradually added to the reaction mixture and grinding continued for further 10 minutes to obtain a homogeneous mixture. Then, the corresponding coupling reagent (20 mmol) was added to the diazonium salt and the grinding continued till the reaction completion. The progress of the reaction was monitored by TLC. The crude product was extracted with ethyl acetate and solid acid was magnetically separated. The solvent was evaporated by rotary evaporator and the crude product purified by recrystallization in ethanol.

### 2.3. Characterization of the synthesized compounds

#### 1-((3-methyl-4-(5-methyl-1*H*-tetrazol-1-yl)phenyl)diazanyl)naphthalen-2-ol (3a):

$^1\text{H}$  NMR ( $\text{CDCl}_3$ , 400 MHz):  $\delta$  2.17 (s, 3H), 2.51 (s, 3H), 6.80 (d,  $J = 10$  Hz, 1H), 7.31 (t,  $J = 8$  Hz, 1H), 7.45 (d,  $J = 8$  Hz, 1H), 7.59 (t,  $J = 8$  Hz, 2H), 7.67-7.75 (m, 3H), 8.50 (d,  $J = 8$  Hz, 1H), 16.20 (s, 1H).  $^{13}\text{C}$  NMR ( $\text{CDCl}_3$ , 100 MHz):  $\delta$  9.10, 17.67, 116.03, 120.01, 122.06, 125.69, 126.80, 128.15, 128.37, 128.99, 129.44, 129.91, 131.05, 133.29, 137.11, 142.20, 145.64, 152.67, 176.69.

#### 1-((4-methyl-2-(5-methyl-1*H*-tetrazol-1-yl)phenyl)diazanyl)naphthalen-2-ol (3b):

$^1\text{H}$  NMR ( $\text{CDCl}_3$ , 400 MHz):  $\delta$  1.74 (s, 3H), 2.73 (s, 3H), 2.74 (s, 3H), 6.34 (s, 1H), 6.78-6.80 (m, 2H), 7.74-7.80 (m, 1H), 7.82-7.99 (m, 1H), 8.01 (s, 1H), 12.61 (s, 1H).

#### 1-((4-methyl-2-(5-methyl-1*H*-tetrazol-1-yl)phenyl)diazanyl)naphthalen-2-ol (3c):

$^1\text{H}$  NMR ( $\text{CDCl}_3$ , 400 MHz):  $\delta$  2.47 (s, 3H), 2.59 (s, 3H), 6.57 (d,  $J = 8$  Hz, 1H), 6.77 (d,  $J = 8$  Hz, 1H), 7.27-7.29 (m, 4H), 8.00 (s, 1H), 8.35 (d,  $J = 4$  Hz, 1H), 8.47 (d,  $J = 8$  Hz, 1H), 15.24

(s, 1H).

**4-((4-(5-methyl-1H-tetrazol-1-yl)phenyl) diazenyl)benzene-1,3-diol (3d):**

<sup>1</sup>H NMR (CDCl<sub>3</sub>, 400 MHz):  $\delta$  2.73 (s, 3H), 6.79 (d,  $J$  = 9.6 Hz, 1H), 7.00 (s, 1H), 7.74 (d,  $J$  = 6.8 Hz, 1H), 8.33 (d,  $J$  = 10 Hz, 2H), 8.74 (d,  $J$  = 8.4 Hz, 2H), 12.61 (s, 2H).

**4-((3-methoxy-4-(5-methyl-1H-tetrazol-1-yl) phenyl) diazenyl)naphthalen-1-ol (3e):**

<sup>1</sup>H NMR (CDCl<sub>3</sub>, 400 MHz):  $\delta$  2.45 (s, 3H), 3.90 (s, 3H), 6.69-6.76 (m, 1H), 7.12-7.48 (m, 2H), 7.62-7.82 (m, 2H), 7.99-8.22 (m, 1H), 8.51 (d,  $J$  = 8 Hz, 1H), 8.66-8.75 (m, 1H), 9.01 (s, 1H), 12.24 (s, 1H).

**4-((4-methyl-2-(5-methyl-1H-tetrazol-1-yl) phenyl) diazenyl)naphthalen-1-ol (3f):**

<sup>1</sup>H NMR (CDCl<sub>3</sub>, 400 MHz):  $\delta$  2.67 (s, 6H), 6.58 (d,  $J$  = 8 Hz, 1H), 6.81 (d,  $J$  = 12 Hz, 1H), 7.74 (s, 1H), 7.81-7.87 (m, 4H), 8.49 (d,  $J$  = 8 Hz, 1H), 8.92 (d,  $J$  = 8 Hz, 1H), 16.12 (s, 1H). <sup>13</sup>C NMR (CDCl<sub>3</sub> + DMSO-d<sub>6</sub>, 100 MHz):  $\delta$  13.38, 22.02, 112.26, 115.87, 117.44, 120.91, 121.83, 122.06, 124.46, 125.93, 126.89, 128.28, 134.92, 139.01, 142.23, 144.94, 149.14, 156.15, 159.26.

**1-((3-methoxy-4-(5-methyl-1H-tetrazol-1-yl) phenyl) diazenyl)naphthalen-2-ol (3g):**

<sup>1</sup>H NMR (CDCl<sub>3</sub>, 400 MHz):  $\delta$  2.49 (s, 3H), 3.95 (s, 3H), 6.79 (d,  $J$  = 8 Hz, 1H), 7.37-7.46 (m, 4H), 7.58 (t,  $J$  = 8 Hz, 2H), 7.73 (d,  $J$  = 8 Hz, 1H), 8.45 (d,  $J$  = 8 Hz, 1H), 16.25 (s, 1H). <sup>13</sup>C NMR (CDCl<sub>3</sub> + DMSO-d<sub>6</sub>, 100 MHz):  $\delta$  13.38, 57.78, 119.91, 121.45, 123.24, 126.43, 128.82, 129.78, 132.93, 136.68, 136.93, 139.24, 142.42, 144.65, 147.57, 154.75, 158.01, 161.12, 165.63.

**4-((3-methoxy-4-(5-methyl-1H-tetrazol-1-yl) phenyl) diazenyl)benzene-1,3-diol (3h):**

<sup>1</sup>H NMR (CDCl<sub>3</sub>, 400 MHz):  $\delta$  2.50 (s, 3H), 3.96 (s, 3H), 6.43 (d,  $J$  = 8 Hz, 1H), 7.05 (s, 1H), 7.11 (d,  $J$  = 8 Hz, 1H), 7.34 (d,  $J$  = 4 Hz,

1H), 7.40 (d,  $J$  = 8 Hz, 1H), 7.44 (s, 1H), 15.39 (s, 1H); 15.89 (s, 1H). <sup>13</sup>C NMR (CDCl<sub>3</sub> + DMSO-d<sub>6</sub>, 100 MHz):  $\delta$  11.98, 51.48, 120.15, 122.47, 124.18, 127.27, 127.89, 131.01, 133.60, 136.42, 141.45, 153.55, 157.62, 163.31, 166.56.

**7-hydroxy-8-((3-methoxy-4-(5-methyl-1H-tetrazol-1-yl)phenyl) diazenyl)-4-methyl-2H-chromen-2-one (3j):**

<sup>1</sup>H NMR (CDCl<sub>3</sub>, 400 MHz):  $\delta$  1.73 (s, 3H), 1.74 (s, 3H), 3.82 (s, 3H), 6.34 (s, 1H), 6.78-6.80 (m, 2H), 7.74-7.80 (m, 1H), 7.82-7.99 (m, 1H), 8.02 (s, 1H), 12.61 (s, 1H).

**4-bromo-2-((3-methoxy-4-(5-methyl-1H-tetrazol-1-yl)phenyl) diazenyl)aniline (3k):**

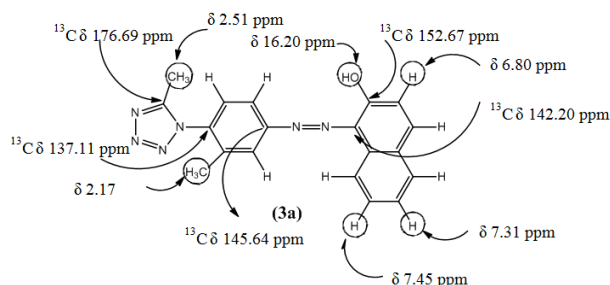
<sup>1</sup>H NMR (CDCl<sub>3</sub>, 400 MHz):  $\delta$  2.46 (s, 3H), 3.85 (s, 3H), 5.30 (s, 2H), 6.65-6.79 (m, 3H), 7.12-7.18 (m, 1H), 7.31-7.53 (m, 1H), 8.23 (s, 1H).

### 3. Results and Discussion

#### 3.1. Chemistry

In continuation with our ongoing efforts for synthesis bioactive natural or synthetic compounds [15], we planned to synthesize tetrazole containing azodyes. Firstly, we prepared 1, 5-disubstituted tetrazole containing amines (**1a-d**) by using reported procedure [16]. Diazonium salts are very important intermediates in the synthesis of organic compounds, especially azodyes. However, the poor thermal stability of diazonium salts, strong acidic conditions, and the difficulty to separate the acidic catalysts from the reaction medium limit the application of these compounds. Hence, we performed the diazotization reaction in the presence of a magnetic solid acid catalyst [17]. Initially, we performed diazotization of 3-methyl-4-(5-methyl-1H-tetrazol-1-yl) aniline (**1a**) in presence of sodium nitrite and Fe<sub>3</sub>O<sub>4</sub>@SiO<sub>2</sub>-SO<sub>3</sub>H solid acid catalyst followed by coupling with  $\beta$ -naphthol (**2a**) to furnish

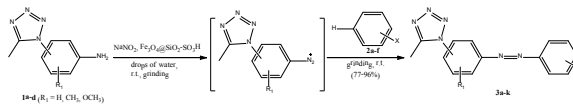
1-((3-methyl-4-(5-methyl-1*H*-tetrazol-1-yl)phenyl)diazonyl)naphthalen-2-ol (**3a**) as a model reaction. The structure of compound is confirmed by  $^1\text{H}$  NMR and  $^{13}\text{C}$  NMR data. The characteristic singlet of O-H is appeared at highly downfield  $\delta$  16.20 ppm, while benzene methyl and tetrazole methyl are appeared at highly upfield as singlet at  $\delta$  2.17 ppm and 2.51 respectively. The remaining C-H peaks are as shown in **figure 1**. The peak at  $\delta$  176.69 ppm is of tetrazole carbon adjacent to methyl. The carbon adjacent to O-H is appeared at  $\delta$  152.67 ppm, while the carbons attached to -N=N- is appeared at  $\delta$  142.20 and 145.64 ppm.



**Fig. 1.** Spectral explanation of 1-((3-methyl-4-(5-methyl-1*H*-tetrazol-1-yl)phenyl)diazonyl)naphthalen-2-ol (**3a**)

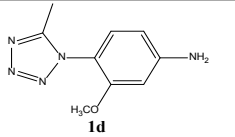
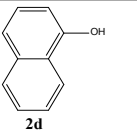
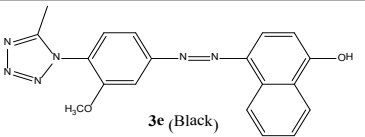
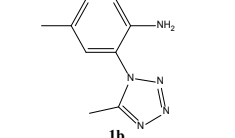
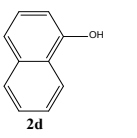
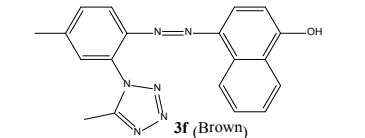
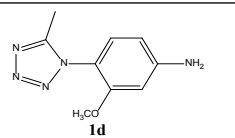
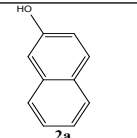
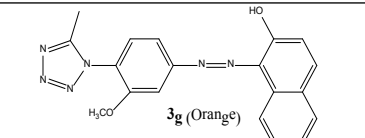
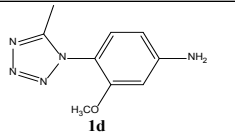
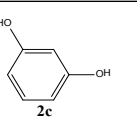
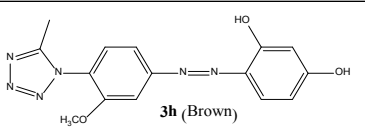
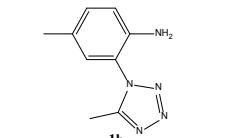
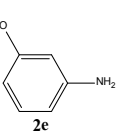
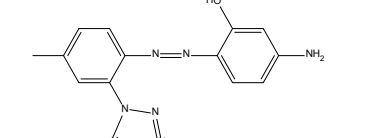
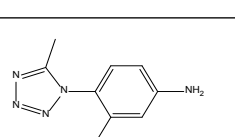
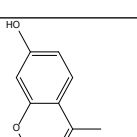
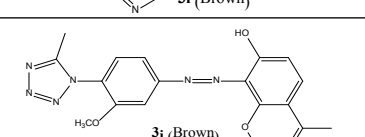

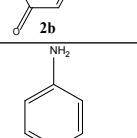
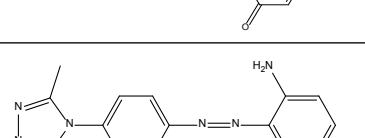
After establishing the suitable optimum conditions, we checked the generality of this method. The reactions of different 1, 5-disubstituted tetrazole amines (**1a-d**) and coupling partners (**2a-f**) to furnished the corresponding tetrazole containing azodye derivatives (**3a-k**) with good yields by the grinding method under solvent free conditions at room temperature (**Table 1**). The structures of all azodye derivatives obtained were confirmed by their spectral and physical data.

**Scheme:** Synthesis of tetrazole containing azodye derivatives.



**Table 1.** Synthesis of tetrazole containing azodye derivatives.

Entry	Tetrazole amines (1a-d)	Coupling reagents (2a-f)	Azodyes (3a-k)	Time (min)	Obs. M. P. (°C)	Yield (%)
1				40	257	96
2				35	165	90
3				45	180	85
4				30	240	77

5				30	230	82
6				40	140	92
7				35	168	87
8				30	262	79
9				45	220	89
10				40	175	88
11				40	135	93

## 3.2. Biology

### 3.2.1. Antibacterial and antifungal activity:

All tetrazole containing azodye synthesized compounds were screened in vitro for the antibacterial and antifungal activity. Antibacterial activity was evaluated against Gram positive and Gram negative bacterial pathogens. *Staphylococcus aureus*, *Bacillus cereus*, *Bacillus megaterium*, *Micrococcus glutamicum*, *Bacillus subtilis* were Gram positive pathogens used in this study. *Escherichia coli*, *Salmonella typhi*, *Shigella boydii*, *Enterobacter aerogenes*, *Pseudomonas aerogenosa*,

*Salmonella abony* were the used Gram negative pathogens. Antifungal activities of synthesized compounds were determined against *Aspergillus niger*, *Saccharomyces cerevisiae*, *Candida albicans* fungal pathogens. Tetracyclin and fluconazol were used as standard antibacterial and antifungal drug respectively. DMSO was used as control solvent. The antimicrobial activity was determined by agar well diffusion method as described by Mancini et al. (2004) [18]. Antimicrobial activity was confirmed if the zone around the agar well was observed. Zones were measured and recorded. The results of compound **3g** and **3k** were as good as the standard drug, so these two compounds might

serve as a good antimicrobial for broad range of bacterial and fungal pathogens. Compound **3k** is very effective (more than standard) against *S.typhi*. It might be due to the presence of electron releasing amino group and bromine on the benzene ring. Another three compounds **3a**, **3b** and **3g** are showing good antimicrobial activity due the presence of tetrazole ring at *para* position and electron donating substituents (-OCH<sub>3</sub> and -CH<sub>3</sub>) at *meta* position. Also, the  $\beta$ -naphthol like substituents are present on -N=N- bond.

**Table 2.** Antibacterial activity of tetrazole containing azo dye derivatives.

Compounds→ Pathogens ↓	3a	3b	3c	3d	3e	3f	3g	3h	3i	3j	3k	Standard
<i>S.typhi</i> ATCC9207	18	16	--	--	--	--	14	--	12	14	27	24
<i>E.aerogenes</i>	08	17	--	12	--	--	06	13	--	--	08	27
<i>B.subtilis</i> ATCC 6633	15	14	12	--	10	--	19	--	14	10	30	25
<i>C.albicans</i> ATCC10231	13	15	--	--	--	--	24	14	--	--	22	25
<i>P.aerugenosa</i> ATCC9027	07	12	--	06	--	--	16	--	--	--	16	33
<i>S.abony</i> NCTC6017	12	11	--	--	09	--	23	13	14	--	20	21
<i>B.megaterium</i> ATCC 2326	11	10	15	--	--	--	15	--	--	--	23	20
<i>E.Coli</i> ATCC8739	18	12	--	10	--	--	15	--	11	13	18	20
<i>S.aureus</i> ATCC 6538	10	14	13	--	--	--	15	--	--	--	24	33
<i>S.boydii</i>	12	12	--	--	15	--	20	--	12	--	25	26
<i>S.cerevisiae</i> ATCC 9763	13	08	--	--	--	--	17	--	--	--	12	20
<i>A.niger</i> ATCC 16404	12	09	--	--	--	--	15	08	--	--	20	25
<i>B.cereus</i>	16	17	08	14	14	--	11	--	13	11	15	28
<i>M.glutamicus</i>	17	18	--	--	--	--	14	05	--	--	14	30

**3.2.2. Minimal inhibitory concentration (MIC):** Minimum inhibitory concentration (MIC) is the lowest concentration of an antimicrobial (compounds) drug that will inhibit

the visible growth of a microorganism after overnight incubation. The MIC was determined for the most potent selected antimicrobial compounds **3a**, **3b**, **3g** and **3k**. The MIC was determined against *B. subtilis* ATCC 6633, *S. typhi* ATCC 9207, *E. Coli* ATCC 8739, *S. abony* NCTC 6017 and *C. albicans* ATCC 10231. The MIC was determined by following of Kumar *et al.*, (2012) [19] with some modification. From the **table 3**, it has been observed that the compound **3k** was found to inhibit the visible growth of *B. subtilis* ATCC 6633, *S. typhi* ATCC 9207, *E. Coli* ATCC 8739 and *C. albicans* ATCC 10231 at low concentration with MIC values 16, 18, 45 and 55  $\mu$ g/ml respectively. While, the compound **3g** was found to inhibit the visible growth of *S. abony* NCTC 6017 at low concentration with MIC value 18  $\mu$ g/ml.

**Table 3.** MIC determination of most potent antimicrobial compounds.

Compounds→ Pathogens ↓	3a	3b	3g	3k	Standard
<i>B. subtilis</i> ATCC 6633	70	70	50	16	3.5 (Tetracycline)
<i>S. typhi</i> ATCC 9207	95	85	55	18	3.0 (Tetracycline)
<i>E. Coli</i> ATCC 8739	70	60	50	45	4.5 (Tetracycline)
<i>S. abony</i> NCTC 6017	90	95	18	30	2.25 (Tetracycline)
<i>C. albicans</i> ATCC 10231	98	90	70	55	12.5 (Fluconazole)

### 3.2.3. Molecular Docking Study:

Molecular docking has become an integral component of the drug discovery toolbox, and its relatively low-cost implications and perceived simplicity of use has stimulated an increasing popularity in academic and industrial research communities. Broadly used in modern drug design, molecular docking methods explore

the ligand conformations adopted within the binding sites of macromolecular targets and imparts knowledge on binding affinities and the associated thermodynamic interactions involved in the intermolecular recognition process that influence the inhibition of the pathogen. Thus, with the aim of rationalizing the significant antimicrobial activity demonstrated by the tetrazole containing azodye derivatives (**3a**, **3b**, **3g** and **3k**) and to understand the molecular basis of their interactions, a molecular docking study was carried out against DNA gyrase subunit b (pdb id:1KZN) as the target receptor. GLIDE (Grid-Based Ligand Docking with Energetics) module integrated in the Small Drug Discovery Suite of Schrödinger molecular modeling software (Schrödinger, LLC, New York, NY) was used to carry molecular docking study [20]. With this purpose, the crystal structure of target enzyme- DNA gyrase subunit b was retrieved from the Protein Data Bank (RCSB) (<http://www.rcsb.org/pdb>). The protein structure was preprocessed for docking simulation using the *Protein Preparation Wizard* which includes eliminating the crystallographically observed water molecules (since they were not found to be conserved in the interaction with the enzyme); appending the missing hydrogens/side chain atoms corresponding to pH 7.0 considering the appropriate ionization states for the acidic as well as basic amino acid residues, assignment of appropriate charge and protonation state and finally energy minimization of obtained structure until the average r. m. s. d. reached 0.3Å. The 2D structures of the most active azodye derivatives (**3a**, **3b**, **3g** and **3k**) to be docked were sketched with the *build* panel in Maestro and converted to energy minimized 3D structures using *ligand preparation tool*. The active site of the enzyme were defined using the *Receptor Grid Generation* panel for which a grid box of 12X12X12Å dimensions around the centroid of the native ligand was generated which was sufficient to explore a larger space of the enzyme cavity. These optimized protein and

ligand geometries were then used as input for the docking calculation against the defined active site using with extra precision (i.e., GlideXP) scoring function to estimate the protein–ligand binding affinities and to rank the docked conformations. The output files generated in the form of the docking poses were visualized and analyzed using the Maestro's Pose Viewer for the key interactions with the residues lining the active site. The optimized ligands were then subjected to docking against the defined active site of DNA gyrase using with extra precision (i.e., GlideXP) scoring function to gauge their binding affinities and mode of interaction. The best docking poses obtained for these ligands were visualized for the mode of binding and analyzed for the key interactions with the active site residues using the Maestro's Pose Viewer utility.

Bacterial DNA gyrase, is a ubiquitous enzyme that play a crucial role in the control of bacterial replicative DNA synthesis. It controls the topological state of DNA within cells and is critical for the essential processes of protein translation and cell replication. This enzyme is composed of two subunits, namely GyrA and GyrB subunits where the A subunit is engaged in interactions with DNA and contains the active site tyrosine responsible for DNA cleavage, while the GyrB subunit encompasses the active site of ATPase required for ATP hydrolysis which is further required for maintenance of DNA topology during the replication process [21]. Inhibition of this enzyme blocks the relaxation of supercoiled DNA and disrupts DNA synthesis leading to cell death. Furthermore, it is exclusive to the prokaryotic kingdom and is essential across bacterial species for the survival of their making it a key drug target for antibacterial chemotherapy. The fluoroquinolones are examples of successful gyrase-targeted drugs, but rapidly emerging resistance to these agents necessitates development of novel compounds with new mechanism of actions against this

enzyme.

A perusal of the ensuing docking simulation revealed that all the four active azodye derivatives (**3a**, **3b**, **3g** and **3k**) could snugly lock into the active of *DNA gyrase* at the co-ordinates close to that of the native ligand with significant binding affinity via formation of several bonded and non-bonded interactions. They produced an average docking score of -8.542 with Glide energy of -43.628kcal/mol. The Glide energy signifies the energy required for the formation

of complex between ligand and the enzyme; lower values signify excellent binding affinity. It also indicates that the ligand is buried inside the cavity of the enzyme. Furthermore a detailed per-residue interaction analysis between these compounds and the residues lining the active site of the enzyme was performed to understand the thermodynamic elements governing the binding of these molecules through which we can speculate the binding patterns in the cavity which is elaborated for **3b** in the next section and is summarized in **table 4** for **3a**, **3g** and **3k**.

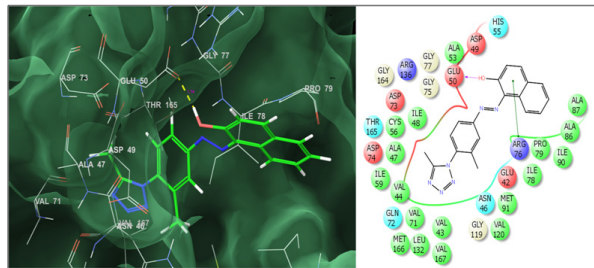
**Table 4.** Quantitative per-residue interaction analysis of the Molecular docking study on *DNA gyrase* enzyme for the most active azodye derivatives.

Code	Glide Score	Glide Interaction Energy (kcal/mole)	Per-Residues interactions			
			Van der Waals (kcal/mol)	Coulombic (kcal/mol)	H-bonds (Å)	Pi-Pi Stacking (Å)
<b>3a</b>	-8.172	-43.568	Val167 (-1.249), Thr165 (-4.125), Arg136 (-1.343), Ser121 (-1.458), Val120 (-1.441), Gly119 (-2.118), Ala96 (-1.723), His95 (-1.048), Ile90 (-2.842), Pro79 (-2.078), Ile78 (-4.152), Gly77 (-1.237), Arg76 (-1.321), Asp73 (-1.79), Glu50 (-1.561), Ala47 (-1.868), Asn46 (-4.135), Val43 (-1.878)	Gly119 (-1.234), His95 (-1.611), Gly77 (-1.272), Arg76 (-2.843), Asp74 (-1.038), Asp73 (-4.062), Glu50 (-4.058)	Glu50 (1.74)	Arg76 (2.404)
<b>3b</b>	-8.882	-43.952	Val167 (-1.376), Thr165 (-1.726), Arg136 (-1.63), Ser121 (-1.545), Val120 (-1.489), Gly119 (-2.002), Ala96 (-1.723), His95 (-1.109), Ile90 (-2.176), Pro79(-4.112), Ile78(-5.392), Gly77(-1.794), Arg76(-4.673), Asp73(-1.88), Glu50(-3.558), Ala47(-1.22), Asn46(-2.664)	Gly119 (-1.456), His95 (-1.921), Gly77 (-1.718), Arg76 (-3.223), Asp74 (-1.678), Asp73 (-1.067), Glu50 (-3.054)	Thr165 (2.21), Gly77 (2.23)	Arg136 (2.193), Arg76 (2.139)
<b>3g</b>	-8.871	-43.159	Val167 (-1.311), Thr165 (-3.123), Arg136 (-1.256), Ser121 (-1.403), Val120 (-2.026), Gly119 (-2.45), Ala96 (-1.111), His95 (-1.120), Ile90 (-1.827), Pro79 (-1.936), Ile78 (-3.351), Gly77 (-1.215), Arg76 (-1.064), Asp73 (-1.131), Glu50 (-1.703), Ala47 (-1.023), Asn46 (-5.159), Val43 (-1.714)	Gly119 (-1.089), His95 (-1.794), Gly77 (-1.367), Asp73 (-6.102), Glu50 (-1.706), Asn46 (-1.442)	Glu50 (1.84)	Arg76 (2.191)
<b>3k</b>	-8.78	-43.834	Val167 (-1.811), Thr165 (-2.183), Arg136 (-1.471), Ser121 (-1.446), Val120 (-1.183), Gly119 (-1.976), Ala96 (-1.723), His95 (-1.113), Ile90 (-1.153), Pro79 (-3.846), Ile78 (-3.343), Gly77 (-1.745), Arg76 (-5.6), Asp73 (-2.621), 72 (-1.214), 71 (-1.871), Glu50 (-3.13), Asp49 (-2.064), Ala47 (-2.281), Asn46 (-3.033), Val43 (-2.152)	Arg136 (-4.727), Gly119 (-1.234), Asp73 (-2.188), Glu50 (-2.076), Asp49 (-1.254), Asp45 (-1.069), Glu42 (-2.079)	Arg136 (2.05), Asp73 (1.92)	Arg76 (2.161)

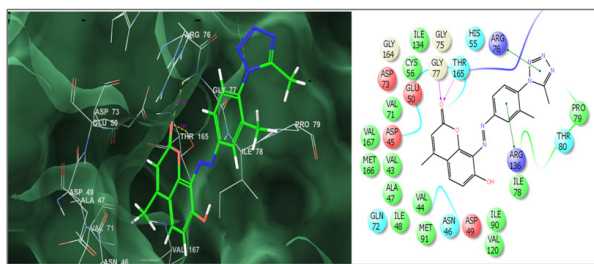


The lowest energy docked conformation (Fig. 3) of **3b** revealed that the compound binds with a significantly higher binding affinity through multiple interactions with the residues in the active site. It binds with a docking score of -8.882 with a Glide energy of -43.952Kcal/mol. Quantification of per-residue interactions with active site indicate that the two halves of the molecule represented by quinolone ring attached to azo group and tetrazolo phenyl ring attached to azo group showed a balanced network of interactions with the active site to hold the molecule within. The compound is stabilized in the active site of *DNA gyrase* through an extensive network of favorable van der waals interactions with Val167 (-1.376 kcal/mol), Thr165 (-1.726 kcal/mol), Val120 (-1.489 kcal/mol), Gly119 (-2.002 kcal/mol), Ile90 (-2.176 kcal/mol), Ile78 (-5.392 kcal/mol), Gly77 (-1.794 kcal/mol), Asp73 (-1.88 kcal/mol), Glu50 (-3.558 kcal/mol), Ala47 (-1.22 kcal/mol), Asn46 (-2.664 kcal/mol) residues through the quinolone ring attached to azo group while the other half i. e. tetrazolo phenyl ring attached to azo group was observed to be involved in a similar network of interactions with Arg136 (-1.63 kcal/mol), Ser121 (-1.545 kcal/mol), Ala96 (-1.723 kcal/mol), His95 (-1.109 kcal/mol), Pro79 (-4.112 kcal/mol) and Arg76 (-4.673 kcal/mol) residues lining the active site of enzyme. The enhanced binding affinity can also be attributed to the significant electrostatic interactions observed via Gly119 (-1.456 kcal/mol), His95 (-1.921 kcal/mol), Gly77 (-1.718 kcal/mol), Arg76 (-3.223 kcal/mol), Asp74 (-1.678 kcal/mol), Asp73 (-1.067 kcal/mol), Glu50 (-3.054 kcal/mol) residues. The interlocking of **3b** is further enhanced by two hydrogen bonds and two pi-pi stacking interactions. A very close hydrogen bonding interaction was observed between the quinolone oxygen and Thr165 and Gly77 residues with a bond distance of 2.21 Å and 2.23 Å. Furthermore two very prominent pi-pi ( $\pi$ - $\pi$ ) stacking interactions were observed first between the

tetrazole ring and Arg76 (2.139 Å), while the second was observed between the phenyl ring and Arg136 (2.193 Å). Such hydrogen bonding and Pi- stacking interactions “anchor” the ligand into the active site of enzyme facilitating the steric and electrostatic interactions. The other active analogues- **3a**, **3g** and **3k** (Fig. 2, 4 and 5 respectively) also exhibited a similar mode of binding and network of bonded and non-bonded interactions. An overview of the per-residue interaction analysis indicates that the mechanical interlocking of these compounds is dominated by the steric complementarity with the active site of *DNA gyrase* as reflected in the relatively higher contribution of favorable van der waals interactions compared to the other components adding to the overall binding affinity. Thus the molecular docking study suggests that these azo derivatives possess excellent affinity for the *DNA gyrase* qualifying them as potential starting points for structure-based lead optimization.

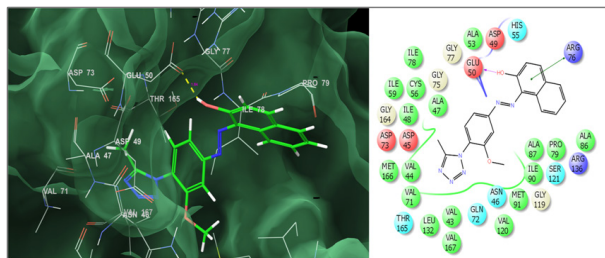


**Fig. 2.** Binding mode of **3a** into the active site of *DNA gyrase* CYP51 (on right side: green lines signify  $\pi$ - $\pi$  stacking interactions while the pink lines represent the hydrogen bonding interactions).

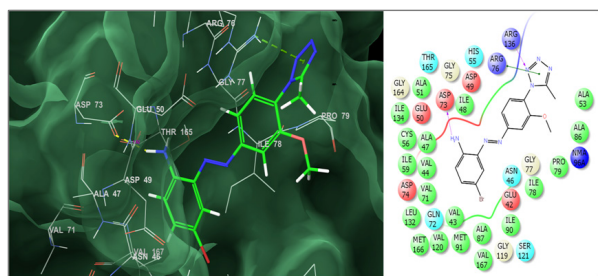


**Fig. 3.** Binding mode of **3b** into the active site

of *DNA gyrase* CYP51 (on right side: green lines signify  $\pi$ - $\pi$  stacking interactions while the pink lines represent the hydrogen bonding interactions).



**Fig. 4.** Binding mode of **3g** into the active site of *DNA gyrase* CYP51 (on right side: green lines signify  $\pi$ - $\pi$  stacking interactions while the pink lines represent the hydrogen bonding interactions).



**Fig. 5.** Binding mode of **3k** into the active site of *DNA gyrase* CYP51 (on right side: green lines signify  $\pi$ - $\pi$  stacking interactions while the pink lines represent the hydrogen bonding interactions).

#### 4. Conclusion

In conclusion, we have reported a series of novel tetrazole containing substituted azodye derivatives. These azodyes were synthesized via diazotization reaction of 1, 5-disubstituted tetrazole containing amines in presence of  $\text{Fe}_3\text{O}_4@\text{SiO}_2\text{-SO}_3\text{H}$  solid acid catalyst followed by coupling reaction. The structures of the compounds were characterized by  $^1\text{H}$  NMR and  $^{13}\text{C}$  NMR spectra. The compounds **3a**, **3b**, **3g** and **3k** have shown very good antibacterial and antifungal activity. Furthermore, the

docking simulations and more specifically the per-residue interaction energy analysis suggest that these compounds have promising affinity for the *DNA gyrase* enzyme making them pertinent starting points for structure-based lead optimization.

#### Conflict of interest

The authors confirm that this article content has no conflict of interest.

#### Acknowledgment

The author PSP is very much grateful to the University Grants Commission, New Delhi for the award of Senior Research Fellowship (SRF). We also thankful to Dr. Babasaheb Ambedkar Marathwada University, Aurangabad for financial support and Schrödinger Inc. for providing the evaluation license of Schrödinger molecular modeling suite to perform the computational studies.

#### References

- Bollu, R.; Banu, S.; Bantu, R.; Gopi Reddy, A.; Nagarapu, L.; Sirisha, K.; Ganesh Kumar, C.; Gunda, S. K.; Shaik, K. *Biorg. Med. Chem. Lett.* **2017**, *27*, 5158.
- (a) Zheng, X.; Sallum, U. W.; Verma, S.; Athar, H.; Evans, C. L.; Hasan, T. *Angew Chem Int Ed.* **2009**, *48*, 2148. (b) Anderson, D. I.; Huges, D. *Nat Rev Microbiol.* **2010**, *8*, 260. (c) Lopes, S. M. M.; Novais, J. S.; Costa, D. C. S.; Castro, H. C.; Figueiredo, A. M. S.; Ferreira, V. F.; Pinho e Melo, T. M. V. D.; da Silva, F. de C. *Eur. J. Med. Chem.* **2018**, *143*, 1010.
- (a) Aufort, M.; Herscovici, J.; Bouhours, P.; Moreau, N.; Girard, C. *Bioorg. Med. Chem. Lett.* **2008**, *18*, 1195. (b) Pereira, D.; Fernandes, P. *Bioorg. Med. Chem. Lett.* **2011**, *21*, 510.
- (a) Vedpathak, S. G.; Momle, R. G.; Ingle, V. S. *World J. Pharm. Res.* **2018**, *07*, 1046. (b) Chfat, H. G.; Ghanim, H. T. *J. Chem. Pharm. Res.*, **2017**, *9*, 93.
- Pesyana, N. N.; Soleimani, D.; Jazani, N. H. *Turk J Chem* **2015**, *39*, 998.
- (a) Yan, Z.; Chong, S.; Lin, H.; Yang, Q.; Wang, X.; Zhang, W.; Zhang, X.; Zeng, Z.; Su, Y. *Eur. J. Med. Chem.* **2019**, *164*, 562. (b) Suresh, A.; Suresh, N.; Misra, S.; Krishna Kumar, M. M.; Chandra Sekhar, K. V. G. *Chemistry Select*,

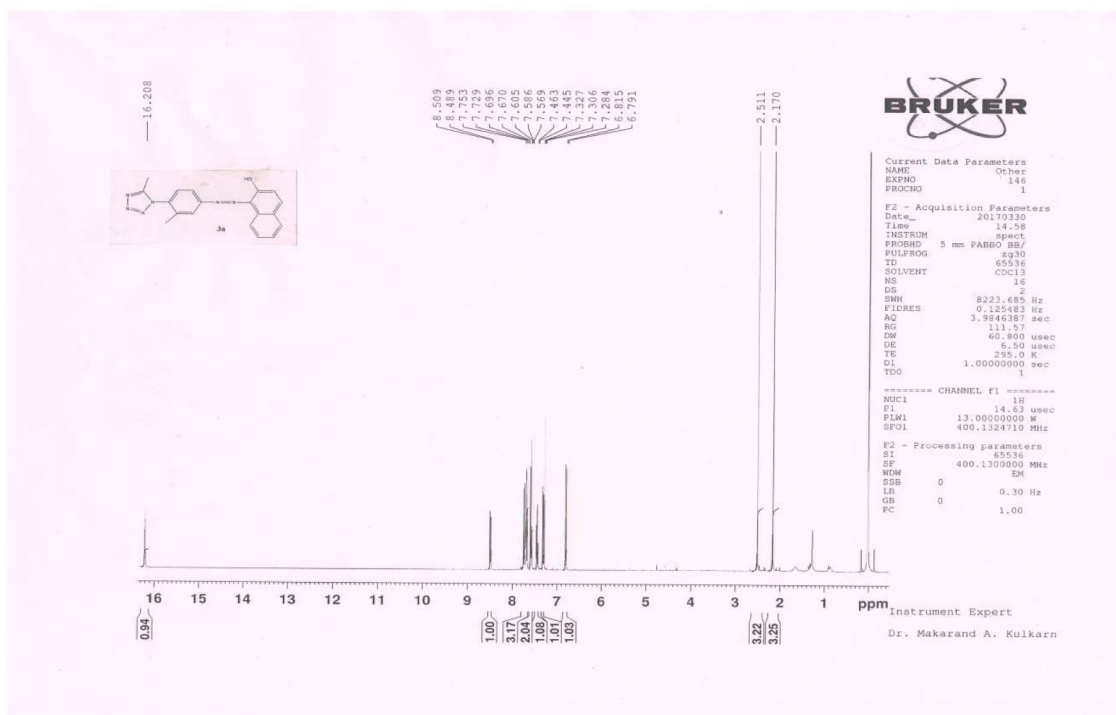


Fig. 1. <sup>1</sup>H NMR (CDCl<sub>3</sub>) spectrum of compound 3a

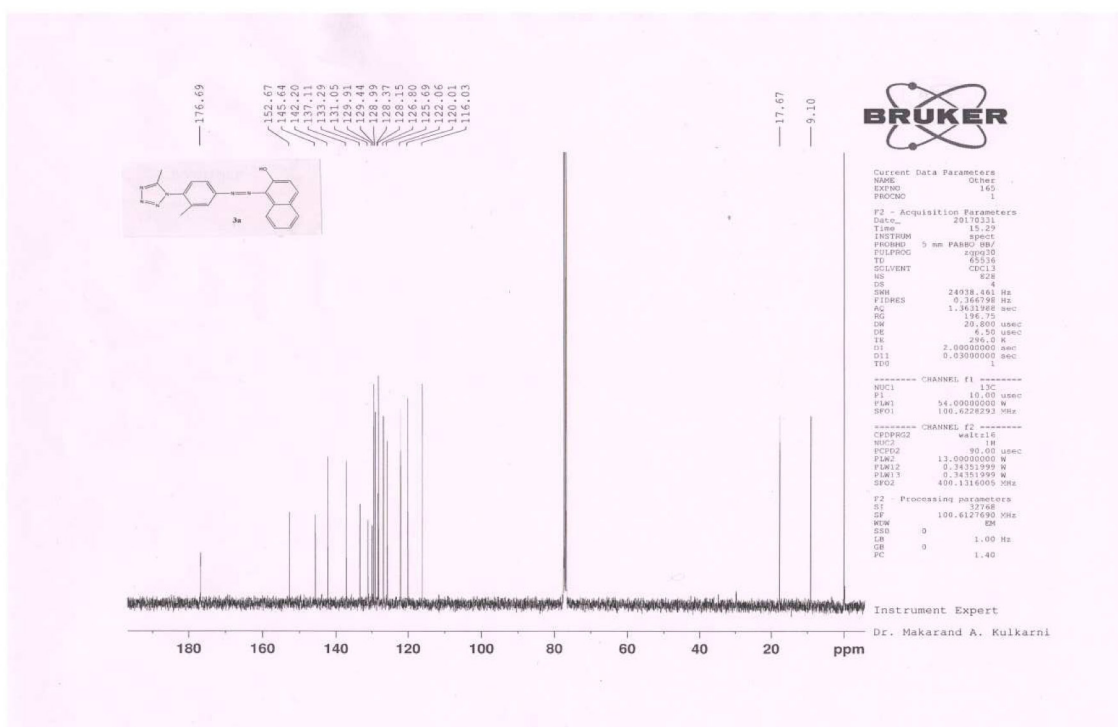


Fig. 2. <sup>13</sup>C NMR (CDCl<sub>3</sub>) spectrum of compound 3a

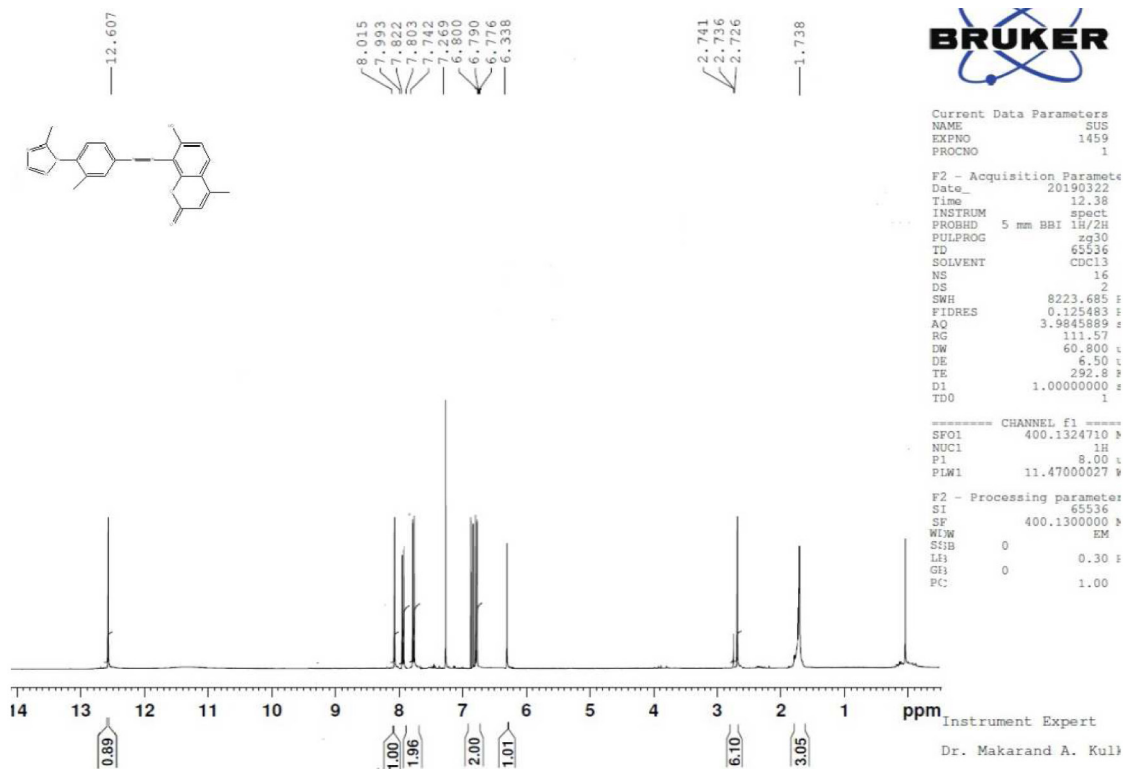


Fig. 3. <sup>1</sup>H NMR (CDCl<sub>3</sub>) spectrum of compound 3b

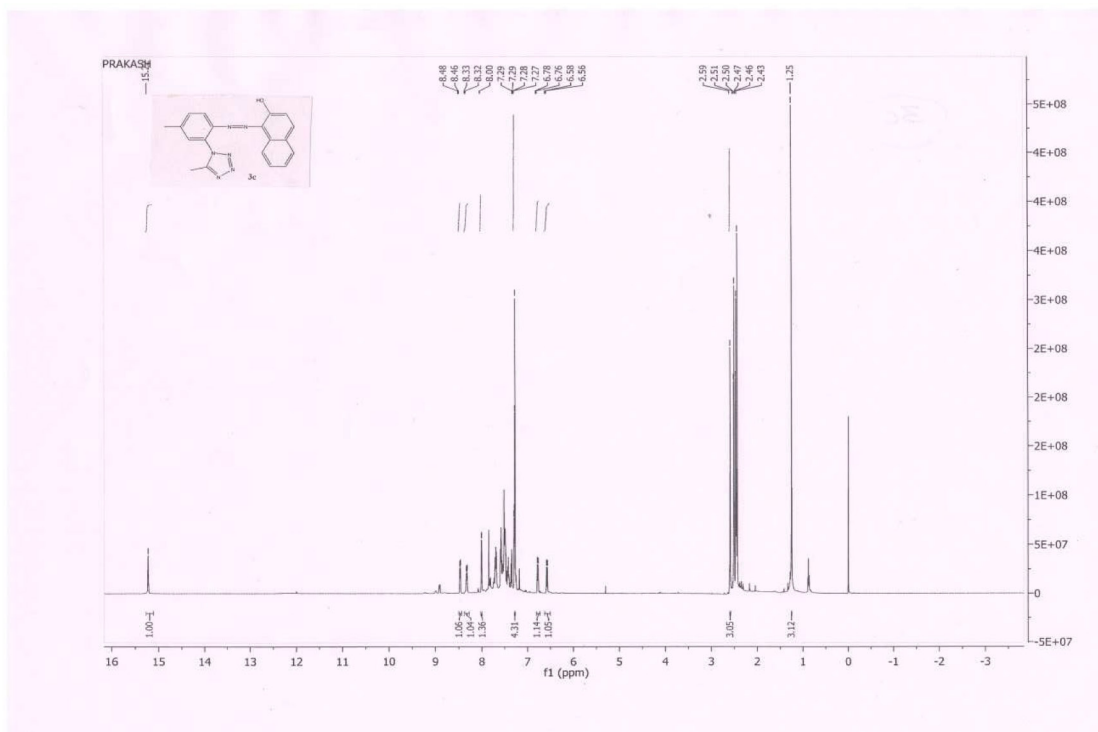


Fig. 4. <sup>1</sup>H NMR (CDCl<sub>3</sub>) spectrum of compound 3c



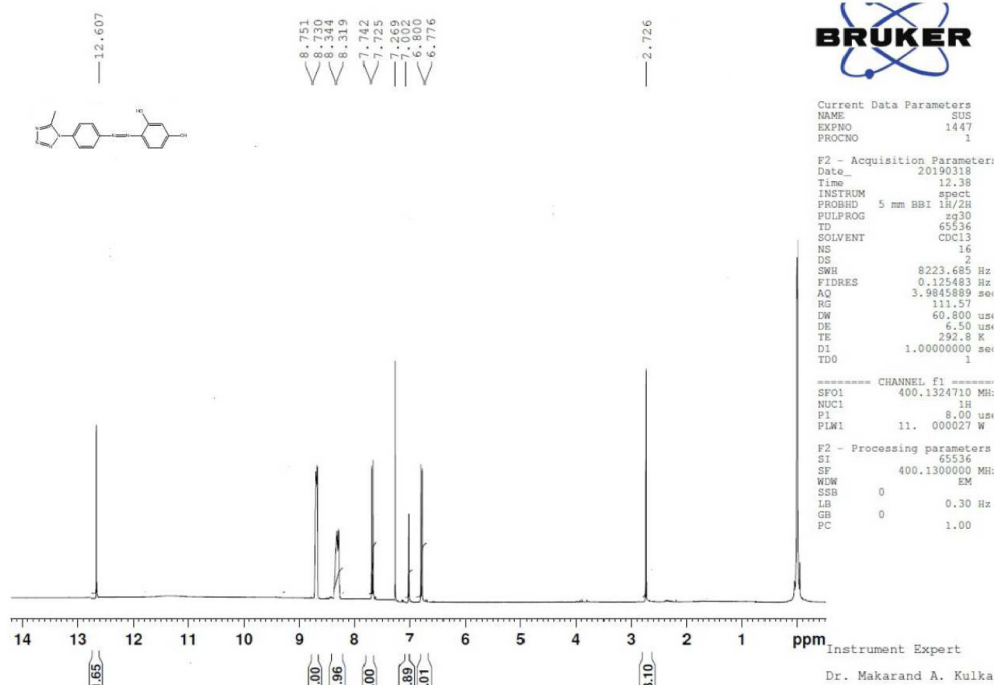


Fig. 5. <sup>1</sup>H NMR (CDCl<sub>3</sub>) spectrum of compound 3d

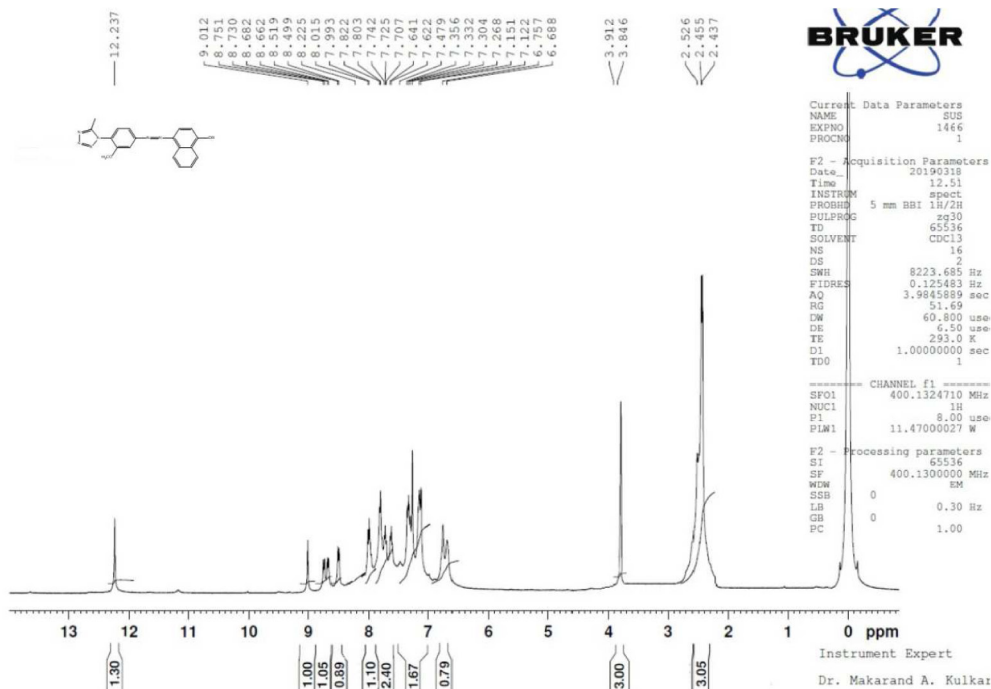


Fig. 6. <sup>1</sup>H NMR (CDCl<sub>3</sub>) spectrum of compound 3e

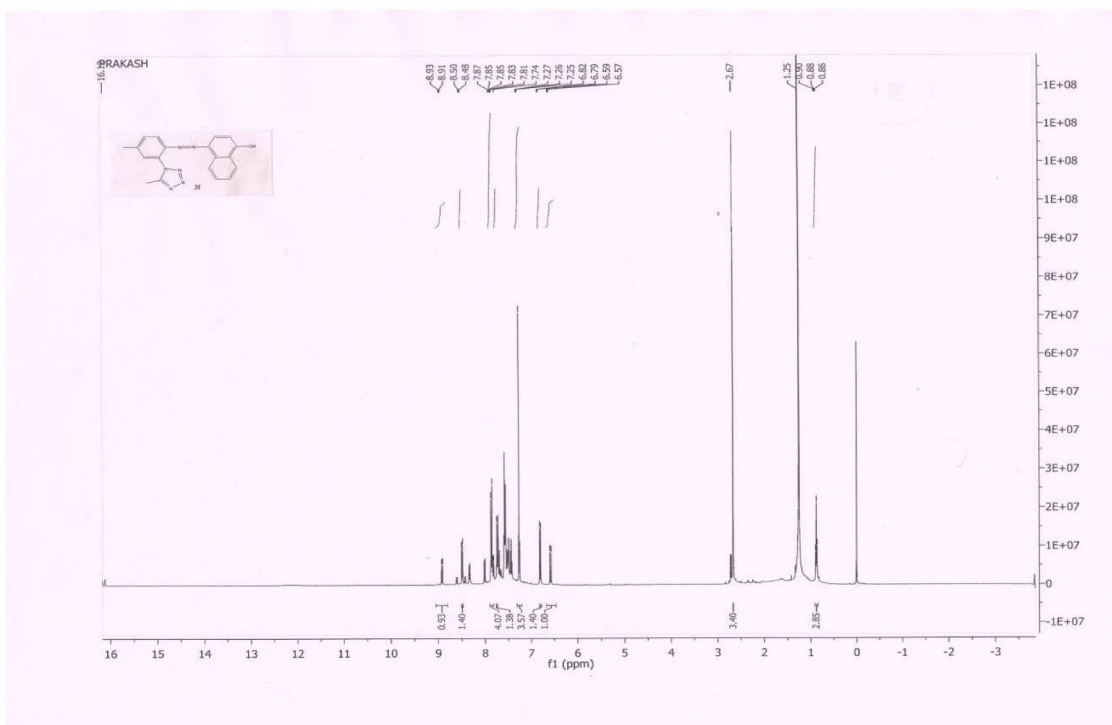


Fig. 7. <sup>1</sup>H NMR (CDCl<sub>3</sub>) spectrum of compound 3f

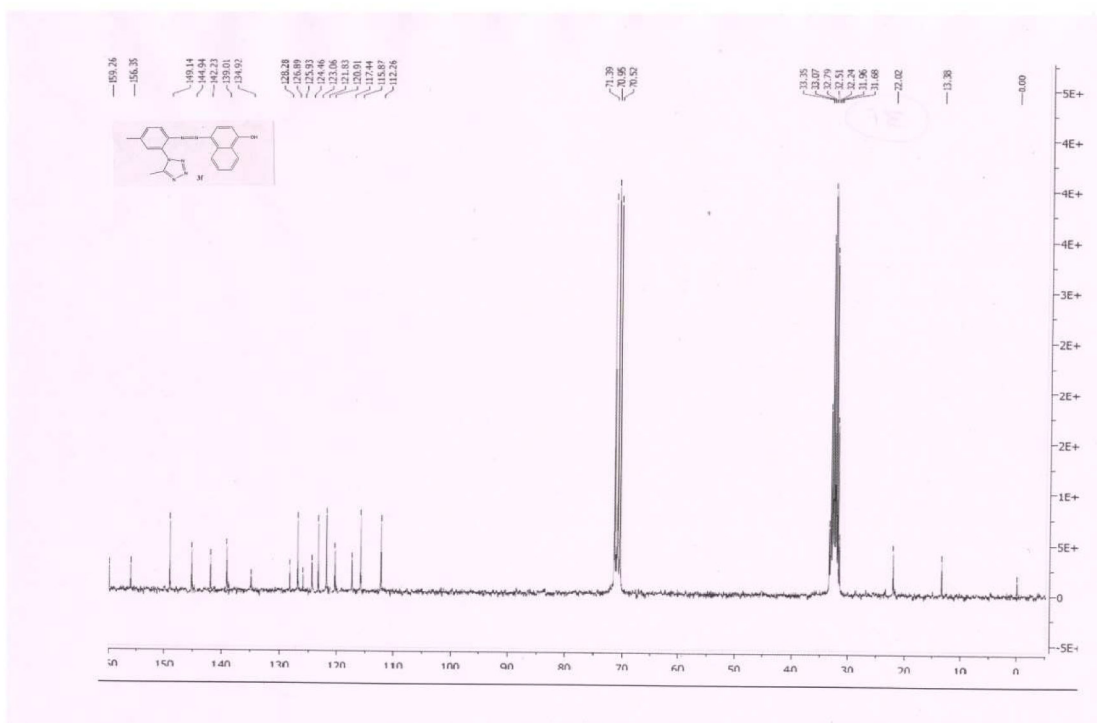


Fig. 8. <sup>13</sup>C NMR (CDCl<sub>3</sub> + DMSO-d<sub>6</sub>) spectrum of compound 3f

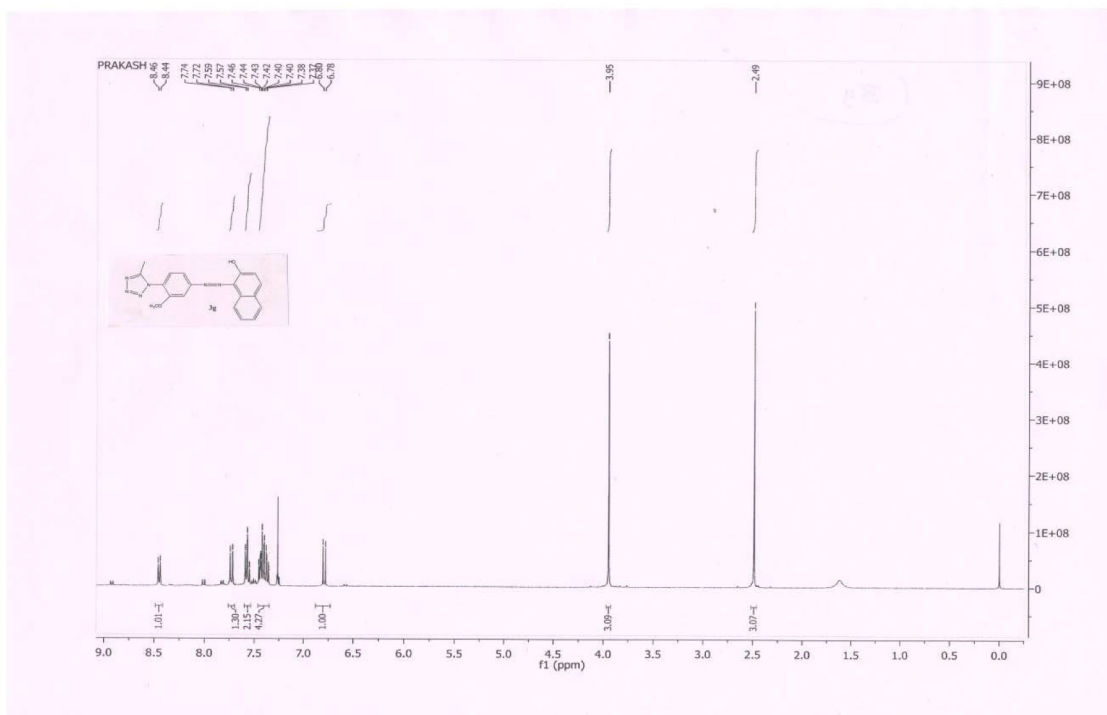


Fig. 9.  $^1\text{H}$  NMR ( $\text{CDCl}_3$ ) spectrum of compound 3g

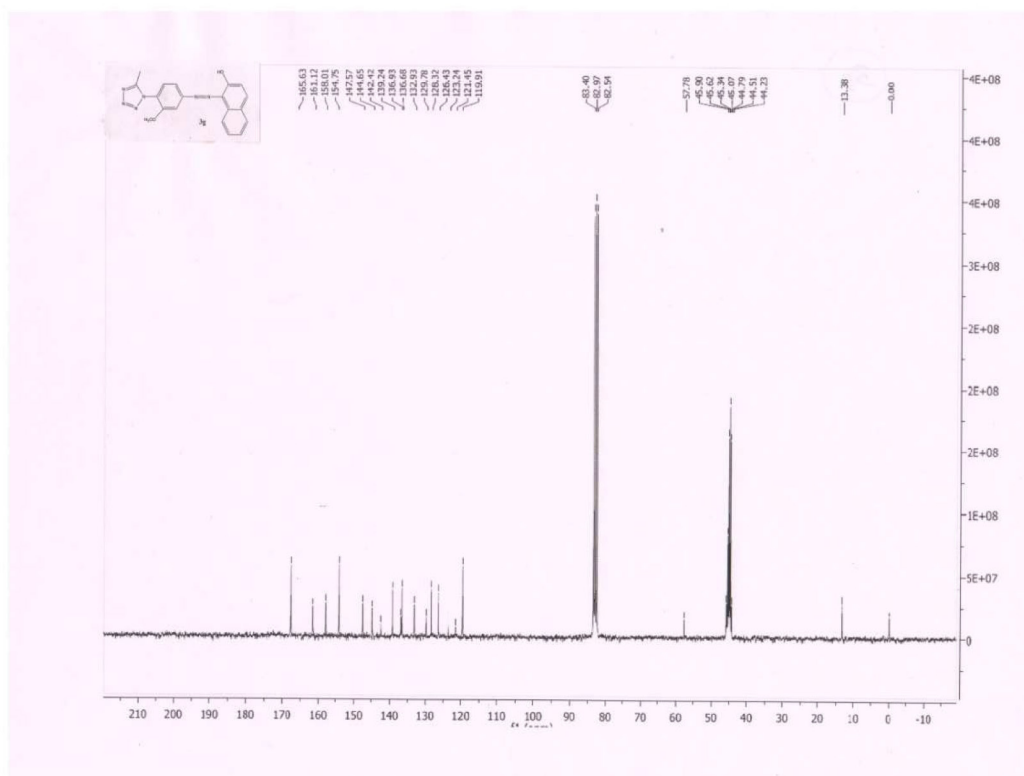
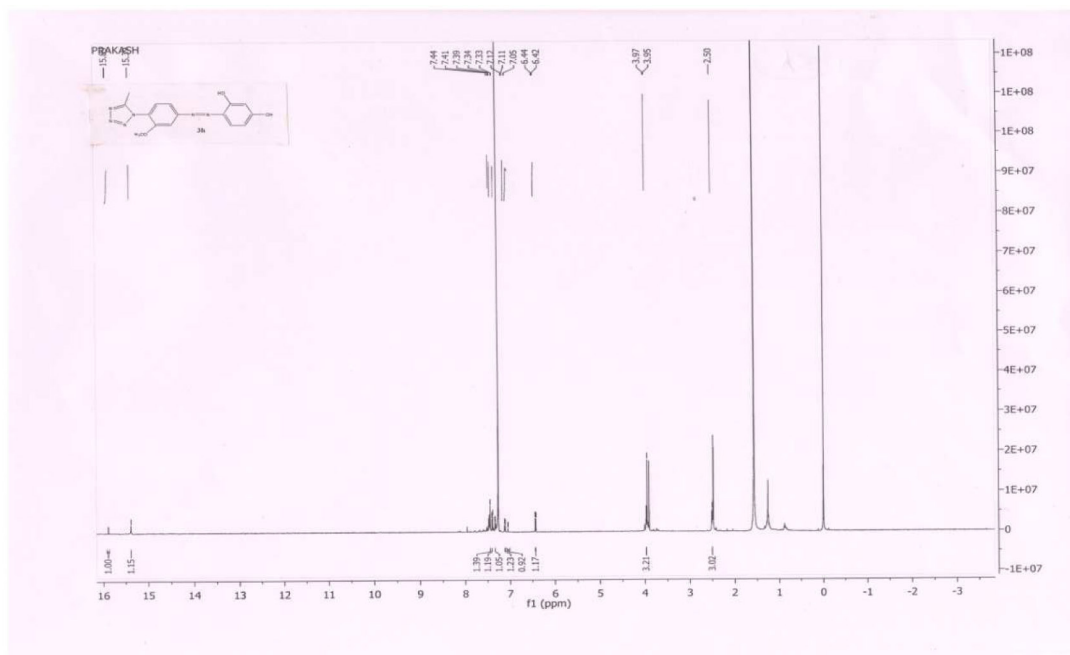
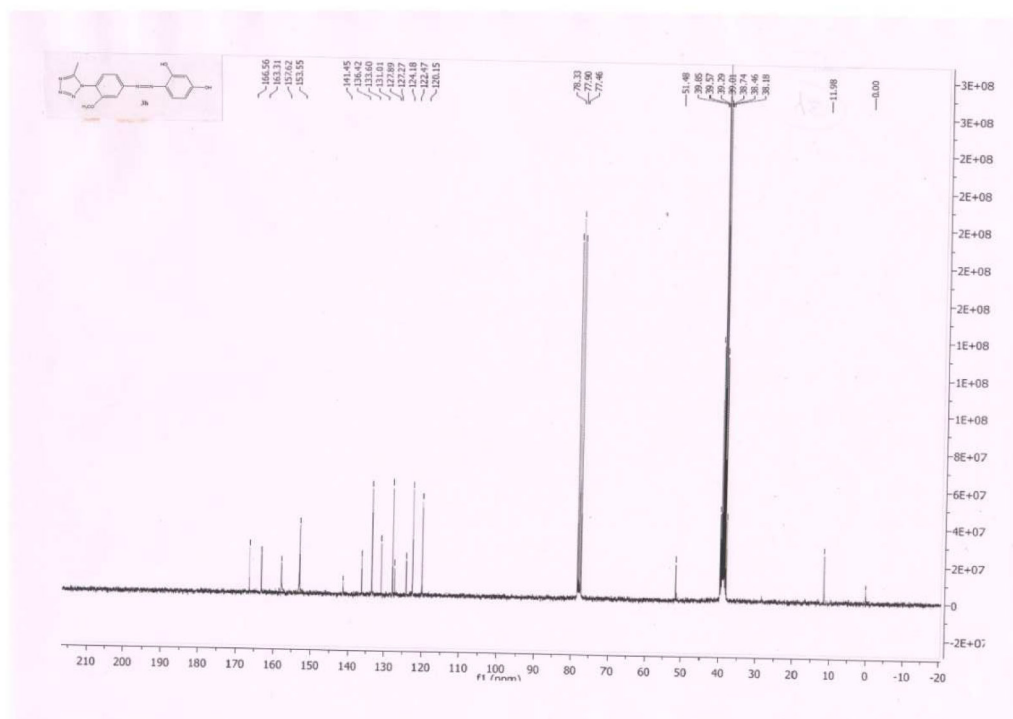


Fig. 10.  $^{13}\text{C}$  NMR ( $\text{CDCl}_3 + \text{DMSO-d}_6$ ) spectrum of compound 3g



**Fig. 11.**  $^1\text{H}$  NMR ( $\text{CDCl}_3$ ) spectrum of compound **3h**



**Fig. 12.**  $^{13}\text{C}$  NMR ( $\text{CDCl}_3 + \text{DMSO-d}_6$ ) spectrum of compound **3h**



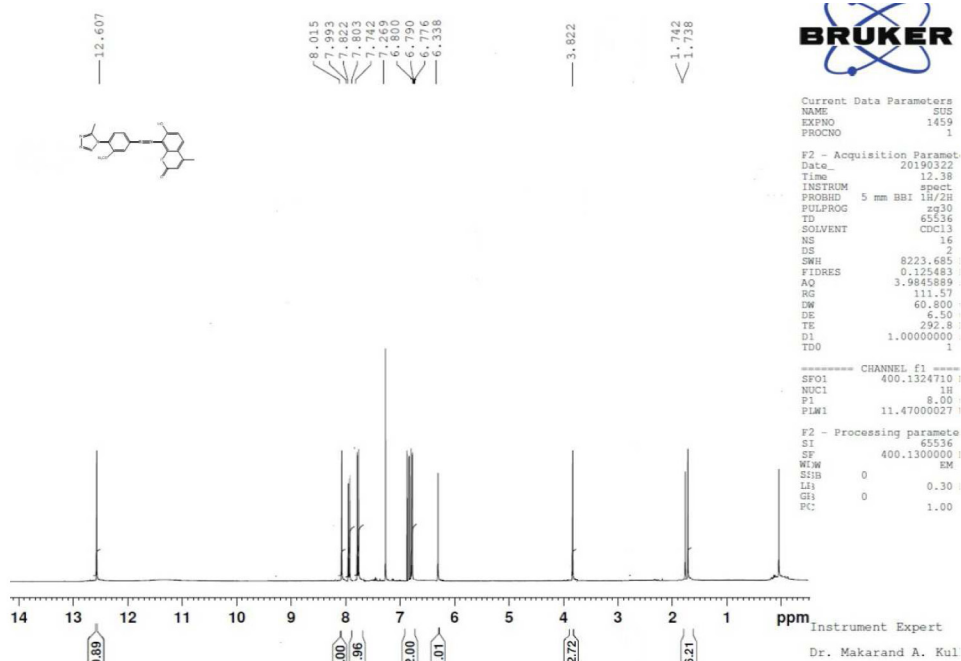


Fig. 13. <sup>1</sup>H NMR (CDCl<sub>3</sub>) spectrum of compound 3j

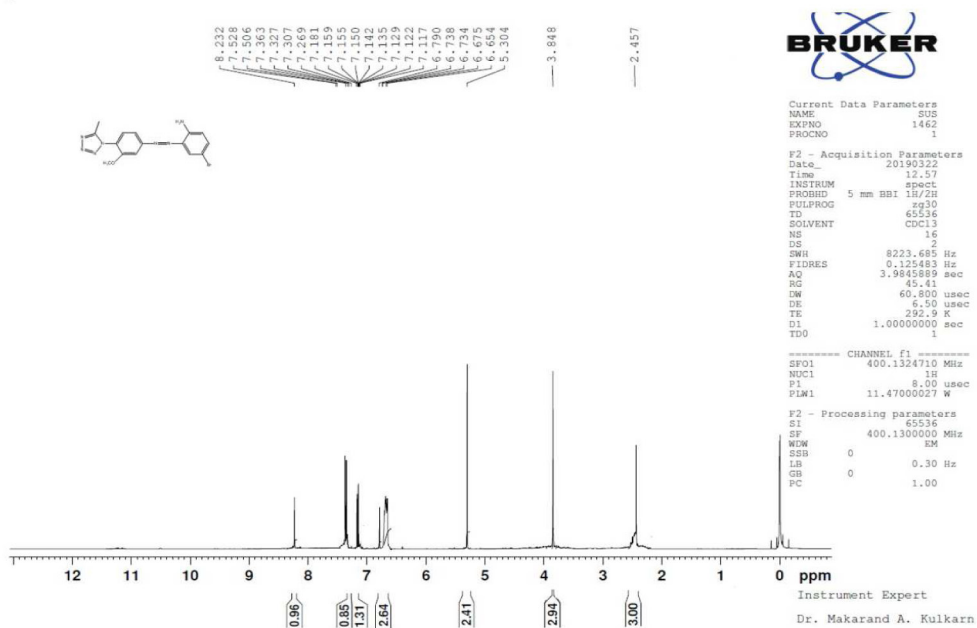


Fig. 14. <sup>1</sup>H NMR (CDCl<sub>3</sub>) spectrum of compound 3k

- 2016, 01, 1705. (c) Hurley, L. H. *J. Med. Chem.* **1989**, 32, 2017. (d) Damia, G.; Borggini, M. *Eur. J. Cancer* **2004**, 40, 2550. (e) Langer, R. *Science* **2001**, 293, 58. (f) Romagnoli, R.; Baraldi, P. G.; Salvador, M. K.; Preti, D.; Tabrizi, M. A.; Brancale, A.; Fu, X. H.; Li, J.; Zhang, S. Z.; Hamel, E.; Bortolozzi, R.; Basso, G.; Viola, G. *J. Med. Chem.* **2012**, 55, 475. (g) Kancheva, V. D.; Boranova, P. V.; Nechev, J. T.; Manolov, I. *Biochimie* **2010**, 92, 1138. (h) Hung, C. Y.; Yen, G. C. *Agric. J. Food Chem.* **2002**, 50, 2993. (i) Koppireddi, S.; Komsani, J. R.; Avula, S.; Pombala, S.; Vasamsetti, S.; Kotamraju, S.; Yadla, R. *Eur. J. Med. Chem.* **2013**, 66, 305. (j) Valko, M.; Leibfritz, D.; Moncol, J.; Cronin, M. T. D.; Mazur, M.; Telser, J. *Int. J. Biochem. Cell Biol.* **2007**, 39, 44. (k) Assous, M. T. M.; Hady, M. M. A.; Medany, G. M.; *Ann. Agric. Sci.* **2014**, 59, 1. (l) Shaghghi, Z. *Spectrochim. Acta A* **2014**, 131, 67. (m) Mohammadi, A.; Ghafoori, H.; Ghalami, C. B.; Rohinejad, R. *J. Mol. Liq.* **2014**, 198, 44.
7. (a) Zarubae, V. V.; Golod, E. L.; Anfimov, P. M.; Shtro, A. A.; Saraev, V. V.; Gavrilov, A. S.; Logvinov, A. V.; Kiselev, O. I. *Bioorg. Med. Chem.* **2010**, 18, 839. (b) Raman, K.; Parmar, S. S.; Singh, S. P. *J. Heterocycl. Chem.* **1980**, 17, 1137. (c) Shngh, H.; Chavez, A. S.; Kapoor, V. K.; Paul, D.; Malhotra, R. K. *Prog. Med. Chem.* **1980**, 17, 151.
  8. (a) Popova, E. A.; Protas, A. V.; Trifonov, R. E. *Anti-cancer Agents Med. Chem.* **2017**, 17, 1856. (b) Koldobskii, G. I.; Ostrovskii, V. A.; *Usp. Khim.* **1994**, 63, 847. (c) Chung, K. T.; Stevens, S. E.; Cerniglia, C. E. *Crit. Rev. Microbiol.* **1992**, 18, 175. (d) Dixit, B. C.; Patel, H.; Desai, D. J. *J. Serb. Chem. Soc.* **2007**, 72, 119.
  9. Upadhayaya, R. S.; Jain, S.; Sinha, N.; Kishore, N.; Chandra, R.; Arora, S. K. *Eur. J. Med. Chem.* **2004**, 39, 579.
  10. Faucher, A. M.; White, P. W.; Brochu, C.; Grand-Maitre, C.; Rancourt, J.; Fazal, G. *J. Med. Chem.* **2004**, 47, 18.
  11. (a) Herr, R. J. *Bioorg. Med. Chem.* **2002**, 10, 3379. (b) Wittenberger S. J. *Org. Prep. Proced. Int.* **1994**, 26, 499.
  12. (a) Kushwaha, P.; Fatima, S.; Upadhyay, A.; Gupta, S.; Bhagwati, S.; Baghel, T.; Siddiqi, M. I.; Nazir, A.; Sashidhara, K. V. *Bioorg. Med. Chem. Lett.* **2019**, 29, 66. (b) Dileep, K.; Polepalli, S.; Jain, N. *Mol Divers.* **2018**, 22, 83. (c) Ye, X. Y.; Yoon, D.; Chen, S. Y.; Nayeem, A.; Golla, R.; Seethala, R.; Wang, M.; Harper, R. *Bioorg. Med. Chem. Lett.* **2014**, 24, 654. (d) Ireland, A. W.; Gobillot, T. A.; Gupta, T.; Seuin, S. P. *Bioorg. Med. Chem.* **2014**, 22, 6490. (e) Ostrovskii, V. A.; Trifonov, R. E.; Popova, E. A. *Russ. Chem. Bull. Int. Ed.* **2012**, 61, 768. (f) Gao, H.; Shreeve, J. M. *Chem. Rev.* **2011**, 111, 7377. (g) Bavetsias, V.; Marriott, J. H.; Melin, C.; Kimbell, R.; Matusiak, Z. S.; Boyle, F. T.; Jackman, A. L. *J. Med. Chem.* **2000**, 43, 1910.
  13. (a) Yousefi, H.; Yahyazadeh, A.; Reza Yazdanbaksh, M. *J. Mol. Struct.* **2012**, 1015, 27. (b) Torres, E.; Bustos-Jaimes, I.; Le Borgne, S. *Appl. Catal. B.* **2003**, 46, 1.
  14. (a) Shaki, H.; Gharanjig, K.; Khosravi, A. *Biotechnol. Prog.* **2015**, 31, 1086. (b) Yazdanbaksh, M. R.; Yousefi, H.; Mamaghani, M.; Moradi, E. O.; Rassa, M.; Pouramir, H.; Bagheri, M. *J. Mol. Liq.* **2012**, 169, 21. (c) Sharma, P.; Rane, N.; Gurram, V. K. *Bioorg. Med. Chem. Lett.* **2004**, 14, 4190.
  15. (a) Phatak, P. S.; Bakale, R. D.; Dhumal, S. T.; Dahiwade, L. K.; Choudhari, P. B.; Krishna, V. S.; Sriram, D.; Haval, K. P. *Syn. Comm.* **2019**, 49, 2017. (b) Kulkarni, R. S.; Haval, N. B.; Kulkarni, J. A.; Dixit, P. P.; Haval, K. P. *Eur. Chem. Bull.* **2019**, 8, 26. (c) Shinde, N. V.; Dhake, A. S.; Haval, K. P. *Orient. J. Chem.* **2016**, 32, 515. (d) Shinde, N. V.; Dhake, A. S.; Haval, K. P. *Der PharmaChemica* **2015**, 7, 251. (e) Haval, K. P.; Argade, N. P. *J. Org. Chem.* **2008**, 73, 6936. (f) Haval, K. P.; Argade, N. P. *Synthesis* **2007**, 2198. (g) Haval, K. P.; Argade, N. P. *Tetrahedron* **2006**, 62, 3557.
  16. Vedpatak, S. G.; Momle, R. G.; Kakade, G. K.; Ingle, V. S. *World J Pharm Res.* **2016**, 5, 1049.
  17. (a) Safari, J.; Zarnegar Z. *RSC Adv.* **2015**, 5, 17738. (b) Hassani, H.; Nasserli, M. A.; Zakerinasab, B.; Rafiee, F. *Appl. Organometal. Chem.* **2016**, 30, 408.
  18. Mancini, I.; Sicurelli, A.; Guella, G.; Turk, T.; Macek, P.; Sepcic, K. *Org. Biomol. Chem.* **2004**, 2, 1368.
  19. (a) Kumar, S.; Dhankhar, S.; Arya, V. P.; Yadav, S.; Yadav, J. P. *J. Med. Plants Research* **2012**, 6, 2754. (b) Dabbagh, H. A.; Teimouri, A.; Chermahini, A. N. *Dyes Pigments*, **2007**, 73, 239. (c) Gorkushko, D. A.; Filimonov, V. D.; Krasnokutskaya, E. A.; Semenischeva, N. I.; Go, B. S.; Hwang, H. Y.; Cha, E. H.; Chi, K. W. *Tetrahedron Lett.* **2008**, 49, 1080. (d) Li, F.; Chen, W.; Dong, P.; Zhang, S. *Biosens Bioelectron* **2009**, 24, 2160. (e) Ramachary, D. B.; Narayana, V. V.; Ramakumar, K. *Tetrahedron Lett.* **2008**, 49, 2704.
  20. (a) Friesner, R. A.; Murphy, R. B.; Repasky, M. P.; Frye, L. L.; Greenwood, J. R.; Halgren, T. A.; Sanschagrin, P. C.; Mainz, D. T. *J. Med. Chem.* **2006**, 49, 6177. (b) Halgren, T. A.; Murphy, R. B.; Friesner, R. A.; Beard, H. S.; Frye, L. L.; Pollard, W. T.; Banks, J. L. *J. Med. Chem.* **2004**, 47, 1750. (c) Friesner, R. A.; Banks, J. L.; Murphy, R. B.; Halgren, T. A.; Klicic, J. J.; Mainz, D. T.; Repasky, M. P.; Knoll, E. H.; Shelley, M.; Perry, J. K.; Shaw, D. E.; Francis, P.; Shenkin, P. S. *J. Med. Chem.* **2004**, 47, 1739.
  21. Collin, F.; Karkare, S.; Maxwell, A. *Appl. Microbiol. Biotechnol.* **2011**, 92, 479.